communications biology

A Nature Portfolio journal

Article

https://doi.org/10.1038/s42003-025-08448-3

Infra-slow scale-free dynamics modulate the connection of neural and behavioral variability during attention

Yujia Ao [1,2], Philipp Klar[2], Yasir Catal [2], Yifeng Wang [1] ✉ & Georg Northoff [2] ✉

The activities of the human brain vary across different timescales, exhibiting scale-free dynamics. Previous research has highlighted the psychological and physiological significance of brain dynamical fluctuations across the Delta to Gamma bands. However, there has been less focus on infra-slow scale-free dynamics, e.g. power law exponent (PLE), and neural variability, e.g. standard deviation (SD), and sample entropy (SE), in mediating brain-behavior connection during attention. In this study, we recruited 49 participants and recorded functional magnetic resonance imaging (fMRI) resting-state and task data during a sustained attention task paradigm to investigate how the three measures—SD, SE, and PLE—modulate the dynamics of behavioral performance. Our findings demonstrate the following: (i) PLE, SD, and SE exhibit differential topographic distribution with a hierarchical structure from sensory to associative networks, during their rest-task modulation. (ii) PLE, SD, and SE show different topographic extensions from visual cortex to default-mode network in their relationship with behavioral variability. (iii) The relationship between SD and SE is mediated by PLE in the empirical data, which (iv) is further confirmed in simulation. Collectively, our results highlight the topographically- and dynamically-layered mechanisms of distinct neurodynamical features during attention processing: scale-free dynamics modulate neural and behavioral variability.

Infra-slow dynamics – How do they modulate cognitive function?

The brain is a highly dynamic system. Understanding its neural activity across various timescales is crucial for unraveling its intricate relationship with cognitive functions and disorders[1–5]. Previous research has predominantly focused on faster frequency ranges [e.g., Theta (4–8 Hz), Alpha (8–12 Hz), Beta (12–40 Hz), and Gamma (40- Hz)] in Electroencephalography/Magnetoencephalography (EEG/MEG) studies[6–9]. Recent investigations have shed light on infra-slow oscillations in the blood-oxygen-level-dependent (BOLD) signal (0.01~0.5 Hz). Some work suggests that these infra-slow BOLD fluctuations predominantly reflect the convolution of high-frequency neural activity—including gamma, as well as theta and alpha bands—with the hemodynamic response function[10,11]. How the infra-slow BOLD fluctuations mediate behavior such performance during an attention task remains yet unclear, though. Addressing this gap in the literature is the goal of our study.

While neuro-vascular effects cannot be excluded[12], emerging evidence suggests the neural basis of the infra-slow BOLD signals, proposed as the dark brain energy by a recent paper[13]. For example, significant correlations between infra-slow BOLD signals and infra-slow local field potential (LFP)/EEG correlations indicate that low-frequency neural coordination underlies large-scale BOLD networks implicated in task performance[14–16]. Furthermore, converging infra-slow electrophysiological, BOLD, and behavioral data reveal that such oscillations across different modalities play a key role in regulating both the integration within and decoupling between concurrently active neuronal communities[17]. Further support comes from studies showing that the activation of the nucleus basalis of Meynert modulates low-frequency global BOLD signals[18]. Collectively, while non-neural factors such as vascular activity and neural-vascular coupling contribute to the BOLD signal (Das et al. 2021), these findings suggest that infra-slow BOLD signals are not merely a byproduct of high-frequency neural activity. This could be further supported by showing how these intrinsic infra-slow neural processes modulate behavioral and cognitive functions; the mechanisms of such neuro-behavioral modulation remain yet to be explored, though[19–23].

Relating infra-slow dynamics to cognitive function confronts one with a methodological challenge. Given that high-frequency brain activity can capture specific cognitive processes within milliseconds, it can measure the effects of single trials lasting 100 to 1000 ms[2,24,25]. This is different in the infra-slow frequency band, which encompasses several to hundreds of

[1]Institute of Brain and Psychological Sciences, Sichuan Normal University, Chengdu, China. [2]Mind, Brain Imaging and Neuroethics Research Unit, Institute of Mental Health Research, Faculty of Medicine, University of Ottawa, Ottawa, ON, Canada. ✉e-mail: wyf@sicnu.edu.cn; georg.northoff@theroyal.ca

seconds, thus aligning with behavior across a multitude of trials in a temporally more continuous way[26]. This raises the question of how the long durations of the infra-slow dynamics can be linked to the usually shorter durations of the cognitive events or trials, such as for instance during attention. Addressing this challenge is needed to better understand the mechanisms how infra-slow dynamics modulate cognition and behavior; that is the main focus of our paper.

Different facets of infra-slow neural dynamics - Scale-free dynamics and variability

Neural timescale refers to the processing duration, from short to long, over which neural activity fluctuates, capturing the duration and temporal structure of brain signals[27]. This broad concept encompasses multiple dynamical properties, such as autocorrelation window[28,29], power spectrum density (PSD)[30], all of which describe different aspects of temporal persistence in neural activity[5].

A key concept in understanding neural timescales is scale-free dynamics, which can be measured by the power-law exponent (PLE)[2,31–33]. This concept of scale-free dynamics describes temporal self-similarity in PSD, where the power distribution of smaller frequency ranges resembles the one of the entire infra-slow frequency ranges. The PLE indicates the distribution of power density/variance across frequencies, e.g., $1/f^{\beta}$: higher PLE (i.e., the value β) reflects more power/variance in lower frequency components and vice versa[31,34,35]. Recent studies have shown that the PLE in the infra-slow frequency range is higher in transmodal association cortices like default-mode network (DMN) and lower in unimodal sensory cortex[36–39]. Furthermore, infra-slow PLE has been linked to various psychological and physiological functions, including aging[40], consciousness[36], task performance[34,41], and rest-task modulation[42,43]. While these findings suggest that scale-free dynamics play a role in cognition and behavior, the precise mechanisms through which scale-free dynamics shape behavioral variability remain yet unclear. One possibility, as suggested by studies on scale-free dynamics[44,45], is that the brain's distribution of slow and fast frequencies may, in a complex corresponding way[46], be manifest on the behavioral and cognitive level and its own variability. However, a critical question remains: How do the different neural dynamic measures (SD, SE, and PLE) interact with one another and thereby shape behavioral fluctuations?

In this study, we aim to investigate this brain-behavior relationship by examining the inter-dependencies between SD, SE, and PLE across multiple large-scale networks and their links to behavioral variability in an attention task. While our approach is primarily correlational, our findings, supported by meditation models and simulation, suggest a hierarchical structure in which PLE acts as a background constraint that modulates the relationship between neural variability (SD and SE) and behavioral fluctuations. Such a layered dynamic organization is in accordance with the recently proposed "Dynamic layer model of brain" (DLB)[5] that has been supported by both fMRI[47,48] and EEG[29] studies; the present paper aims to show the key relevance of such a dynamically layered organization for a specific cognitive process, namely attention.

In addition to its scale-free dynamics, the brain's neural dynamics exhibit significant variability across different timescales[28,35,49]. The conception of neural variability describes the degree of change of neural activity across time[50]. The simplest and most common measure of neural variability is the standard deviation (SD), representing the distributional width of a neural time series[50]. It has been applied in various functions in neuroimaging studies including cognition[51,52], consciousness[42,53–55], mental disorders[56,57], aging[40,58], and various other functions and processes[50]. This makes neural variability a promising candidate to link neural and behavioral dynamics in the infra-slow frequency range[50,52,59–62].

The sample entropy (SE) estimates neural variability and specifically its predictability by analyzing the distribution of temporal patterns based on information theory, i.e., the complexity[50,63]. SE has been validated and effectively used in fMRI studies[48,64–66]. For instance, SE of the BOLD signal was demonstrated to be related to the task performance[67], aging[68], and mental disorders such as attention deficit and hyperactive disorder (ADHD)[69]. However, the relationship between variance-based SD and information-based SE, and how they are mediated by their underlying scale-free dynamics, as measured by the PLE, remains yet unclear.

From neural to behavioral dynamics – what are the mediating mechanisms?

Like brain dynamics, behavioral dynamics exhibit temporal variability and share temporal patterns with neural activity[5,70]. For example, Ding and colleagues showed that MEG signals at different timescales concurrently tracked the timescales of different linguistic units such as words, phrases, and sentences[71]. Evidence supports that both sustained attention and neural activity in the frontoparietal network exhibit theta rhythm[6,25,72]. The steady-state evoked potential (SSEP) findings revealed that the brain's neural entrainment to rhythmic stimuli, strongly supporting the alignment of brain and behavior[73,74].

Together, these studies revealed a direct brain-behavior connection through entrainment and alignment in the high-frequency range of EEG/MEG. This leaves open the dynamic mechanism of such brain-behavior connection in the infra-slow frequency range. A few individual fMRI studies have begun to explore this question, suggesting a potential direct relationship in this slower frequency domain. For instance, two studies using a simple reaction time task with fixed trial intervals at frequencies of 0.0625 Hz and 0.125 Hz found increased PSD at corresponding frequencies, which is known as low-frequency steady-state brain response (lfSSBR)[75,76]. A recent study using an n-back task also revealed that reaction time and working memory capacity are related to BOLD activity at the same frequency as stimuli presentation[47]. These studies suggest that behavior, neural activity, and task stimuli share their temporal structure in the infra-slow frequency range—behavior and brain activity may thus share the same infra-slow timescale, e.g., "common currency"[70] in their fluctuations. Such commonly shared fluctuations allow linking all three levels, external input, internal neural activity, and the subsequently resulting behavior. However, despite these advances, the mechanism through which infra-slow neural dynamics process the temporal features of the input stimuli and how that, in turn, shapes behavior across different timescales, remains yet unclear.

Sustained attention, a fundamental psychological function, exhibits fluctuations ranging from seconds to minutes[77]. These attentional fluctuations occur within the infra-slow frequency range (0.01–0.1 Hz) of neural activity and cognitive performance, highlighting the close interplay between infra-slow neural dynamics and attentional dynamics[17,23,77]. For example, recent studies have revealed that infra-slow oscillatory transcranial direct current stimulation (tDCS) enhances performance in sustained attention tasks, advancing research on the relationship between neural dynamics and fluctuations of sustained attention[78]. Thus, investigating sustained attention fluctuations may provide important insights into the mechanisms of how infra-slow neural dynamics mediates cognitive function, e.g., the dynamical brain-behavior connection.

Aims, hypotheses, and procedures

In this study, we utilized the Gradual-onset Continuous Performance Task (GradCPT) paradigm to measure moment-to-moment attention fluctuations by constantly recording reaction time at intervals of 1200 ms (see Fig. 1 top-left)[79]. A key advantage of this paradigm is its alignment with the fMRI sampling rate, as the repetition time (TR) of our fMRI acquisition was 800 ms. This results in an approximate ratio of 2 RT values per 3 BOLD volumes, enabling simultaneous exploration of brain and behavioral dynamics within the same infra-slow frequency range[79]. Through this approach, we aim to connect neural and behavioral dynamics, with three specific objectives and steps (conceptualized in Fig. 1):

Step 1: Investigation of the rest-task modulation in GradCPT paradigm for SD, SE, and PLE in the infra-slow frequency range. We primarily hypothesized that all three measures show task-related modulation in visual and somatomotor networks, the unimodal cortex, which are thought to primarily process visual-motor inputs as required in our task[28,80].

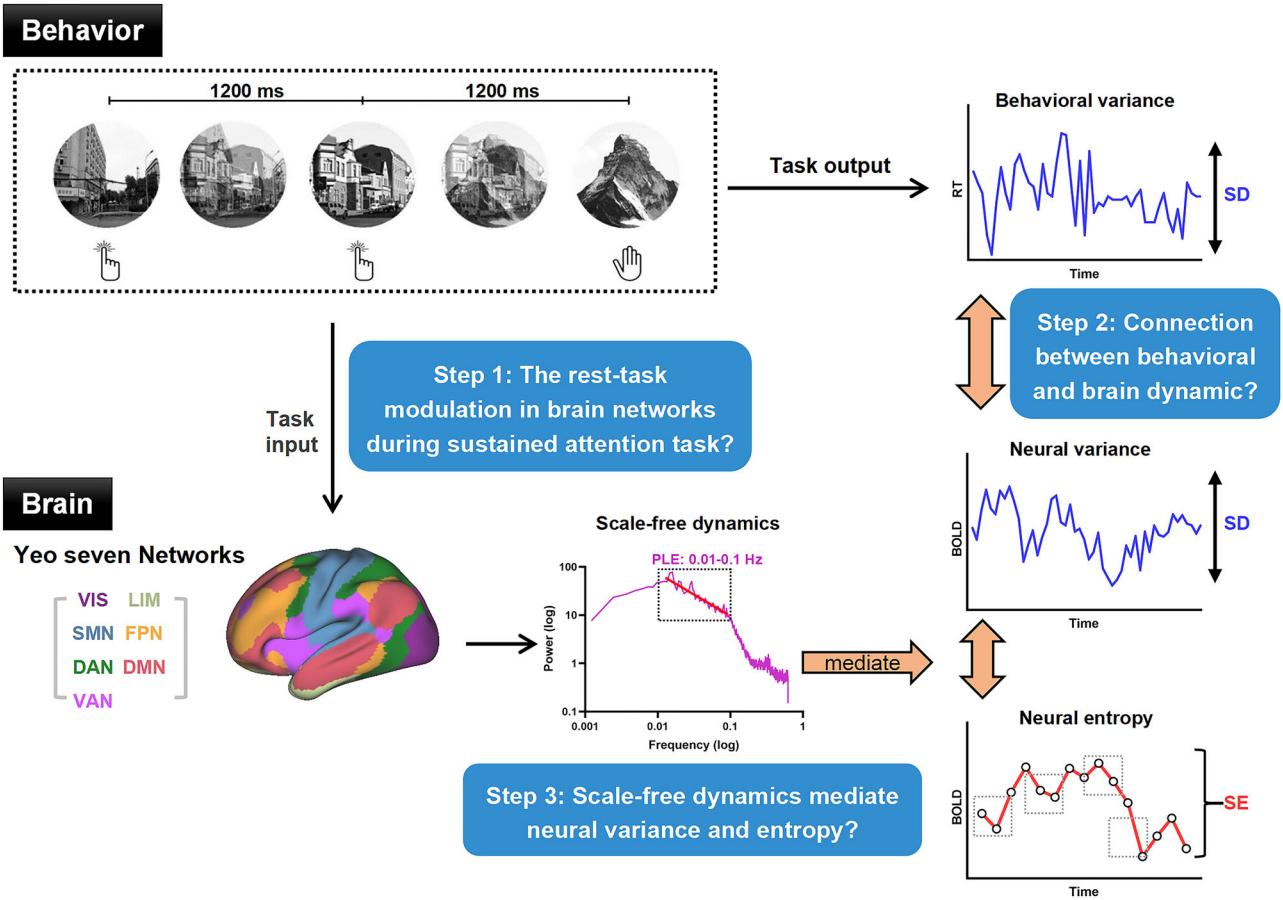

Fig. 1 | Concept and procedure of the current study. This Figure contains three key steps: (1) Examining the sustained attention task modulation by detecting the rest-task difference in three measures; (2) Investigating the connection between behavioral and brain dynamics by correlating neural and behavioral measures; (3) Conducting mediation analysis to assess PLE mediation on the relationship between SD and SE.

Additionally, we hypothesized that the dorsal and ventral attention networks, important in attentional control functions, will participate in such dynamic task modulation reflecting the cognitive demands of our sustained attention paradigm[81].

Step 2: Investigation of the connection between neural and behavioral dynamics. We hypothesized that SD and SE of the BOLD signal relates to behavioral variance (SD) although in distinct ways in the networks like the visual, somatomotor, and attention networks that are known to mediate the attention task[81]. We also suppose that the PLE will mediate the brain-behavior relationship in sensory input regions like the visual network, given its key role in input processing[33,36,37,39,44].

Step 3: Investigation of the relationship of BOLD signal's SD with SE and PLE. We primarily hypothesized the three measures to reflect different facets or layers of neural dynamics as suggested in the 'Dynamic layer model of brain'[5]. This may be reflected by their topographical differences along for instance, lower-order sensorimotor and higher-order cognitive networks[36–38]. Furthermore, we hypothesize that the PLE, as a more comprehensive and most basic or fundamental measure operating in the neural background[48], mediates the relationship of neural SD and SE in the neural and behavioral foreground. This step involves empirical data analysis and simulated data analysis to assess the mathematical relationship of SD and SE in dependence on varied PLE values.

Results

Differences in neural dynamics between rest and task states occur mainly in sensorimotor and attention-related cortices

This study primarily aimed to examine the differences between rest and task states using three measures of brain dynamics: SD, SE, and PLE. Figure 2A illustrates the topographical distributions of these measures during both resting and task states. Notably, the spatial distributions of SD, SE, and PLE are significantly different from each other. For instance, during the task state, SD and PLE exhibit elevated distributions in frontoparietal network (FPN) but diminished distributions in somatomotor network (SMN) (see Fig. 2A, and Supplementary Fig. 1 for statistics).

Crucially, the significant t-test differences [$n = 49$, $p < 0.05$, false discovery rate (FDR) corrected] between rest and task states in these measures are consistently manifested in and overlap with each other across all three measures within unimodal regions and attention-related networks, specifically the visual network (VIS), SMN, dorsal attention network (DAN), and ventral attention network (VAN) (Figs. 2B and 3). Although the changes in SD within DMN are significant, the effect is minimal when compared to the SD changes observed in the unimodal and attention-related cortices. Furthermore, the study found a decrease in the values of SD and PLE from rest to task in those networks, while SE increased in the same regions; this suggests that SE may inversely influence behavioral outcomes during our attention task.

Together, these findings reveal a consistent pattern of rest-to-task changes across all three dynamical measures (SD, SE, and PLE) in unimodal networks. However, in high-order networks such as the default mode network (DMN), only SD exhibits a task-related increase, while SE and PLE follow different patterns (schematized in Fig. 2C). Importantly, this pattern was also observed after task regression (Supplementary Table 1), indicating that in unimodal networks the three measures converge in their responses to the task, whereas in higher-order networks (FPN and DMN) their changes diverge. Moreover, it shall be noted that we observed task-related decreases in both PLE and SD, whereas SE

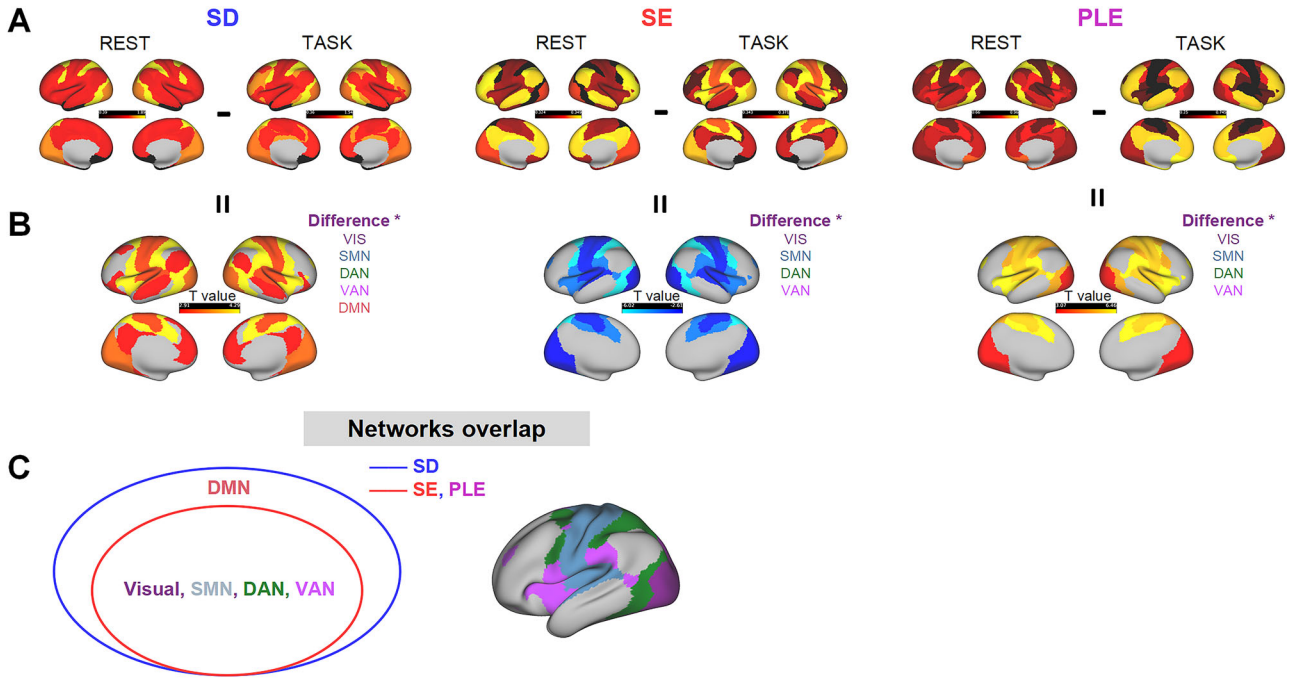

Fig. 2 | Rest-task difference of SD, SE, and PLE. A The topographies of SD, SE, and PLE in resting and task states. **B**: Paired t-test results for rest-task differences within subjects ($n = 49$, $p < 0.05$, FDR corrected). **C** Schematics for the overlapped networks in three measures.

exhibited the opposite pattern, showing a task-related increase across all examined networks.

From neural to behavioral dynamics: the differentiation of brain-behavior relation through the distinct neural dynamics of SD, SE, and PLE

We next explored how the three dynamic measures correlate with behavioral performance as indexed by the SD of the RT. Figure 4A demonstrates the Pearson correlations between the three BOLD measures and RT across the seven networks at the group level ($n = 49$, FDR corrected for 21 comparisons).

Specifically, PLE displayed significant positive correlations exclusively within the VIS, a key network predominantly involved in processing visual stimuli in our attention paradigm. A different pattern was observed in SE, which showed negative brain-behavior correlations in both the sensorimotor cortex and attention-related networks, including VIS, SMN, DAN, and VAN.

Finally, SD of RT positively correlated with BOLD SD in networks overlapping with SE but also in DMN, as shown in Fig. 4B. This correlation remained significant in the task-regressed data (Supplementary Table 2). Supplementary Fig. 2 shows that the distributions of SD, SE, and PLE values are approximately Gaussian with a wide range, supporting the validity of our correlation analysis. We also calculated Spearman's rank correlations (Supplementary Table 1). Although the Spearman correlations for SD and SE in the VIS and SMN (and for PLE in VIS) were nominally significant ($n = 49$, $p < 0.05$), none survived correction for multiple comparisons. This suggests that the RT–BOLD relationship is primarily linear rather than monotonic or non-linear. Moreover, the broad data distributions (Supplementary Fig. 2) justify using Pearson's correlation to capture the full variability in the data.

We also examined both Pearson's and Spearman's correlations between the three BOLD measures and additional behavioral metrics, including mean RT, number of commission errors, and number of omission errors (Supplementary Tables 3–9). None of these correlations survived multiple comparison correction, indicating that the variability-based BOLD measures are primarily associated with behavioral variability, rather than with the mean behavioral performance as averaged across the single trials. Overall, we show a linear relationship between the variability of the BOLD signal and the variability of the RT.

Together, these findings suggest a hierarchical topographic-dynamic structure of brain-behavior connections that extend from PLE to SE and SD, moving from the visual network over attention-related networks to higher-order networks like DMN. This pattern suggests distinct roles of the three measures of the dynamics of BOLD signal in mediating behavioral dynamics.

From the neural background to the connection of neural and behavioral foreground: PLE mediates the relationship between BOLD variability and behavioral variability

Next, we raised the question about the role of PLE in mediating the relationship between neural and behavioral dynamics in VIS, which showed significant correlation between brain and behavior in all our three dynamical BOLD measures. Given that a previous study[48] showed a mediating role of PLE, we first tested whether the relationship between BOLD and behavioral SD was mediated by PLE (Fig. 4B). This indeed yielded a partial mediation effect, showing that PLE is a key factor in mediating the transition from neural variability to behavioral variability. In contrast, BOLD SE showed no significant PLE mediation effects with behavioral SD. In the task-regressed data, we found full mediation, further underscoring PLE as a fundamental background linking neural variability to behavioral variability.

Together, these findings demonstrate the key role of scale-free dynamics in operating in the neural background that facilitates the more foreground connection of BOLD variability with behavioral variance.

Scale-free dynamics operate as neural background for neural foreground SD and SE: their relation is strongest in the pink noise regime (empirical and simulated data)

Our findings showed that PLE, as a background index, mediates the relationship from neural variability to behavioral variability (Fig. 4). This raises the question of whether PLE also operates in the neural background for the relationship of SE and SD on a purely neuro-dynamical level. To test this hypothesis, we test the relationship between PLE and other dynamical measures such as SD and SE in the seven networks.

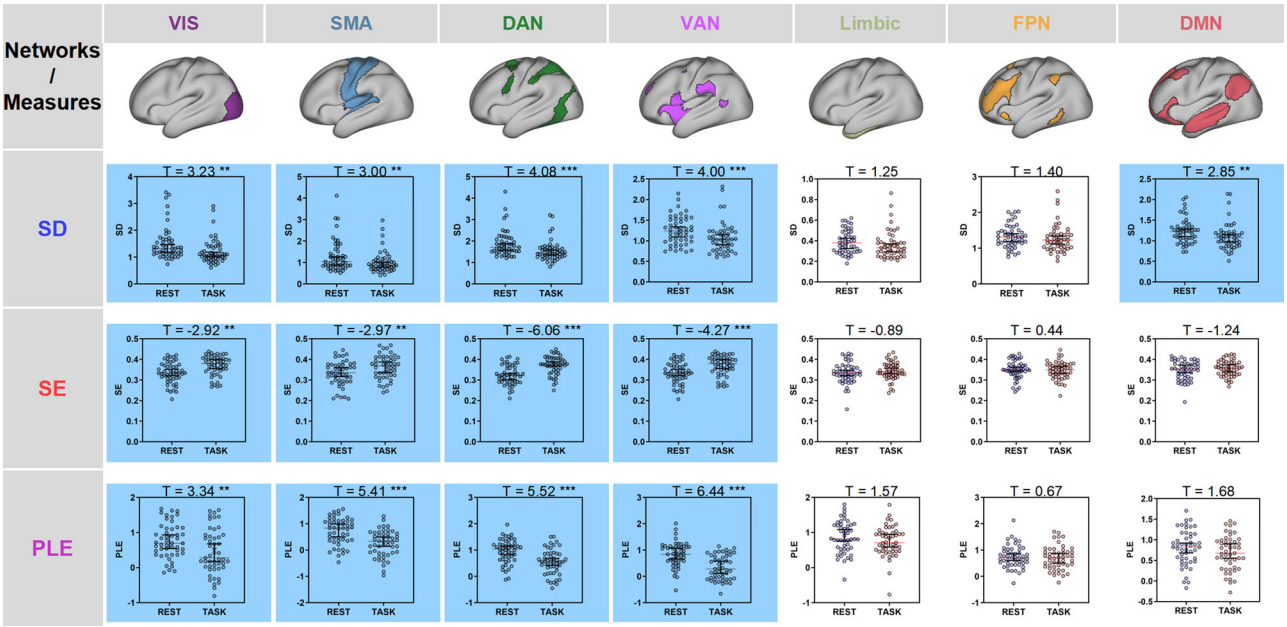

Fig. 3 | The statistics of rest-task differences for three measures in seven networks. Error bars in dot-plots indicate the median value with 95% CI of the measure across participants (n = 49). Significance levels are denoted as follows: $^{*}p < 0.05$, $^{**}p < 0.01$, $^{***}p < 0.001$, $^{****}p < 0.0001$.

As shown in Fig. 5A, we first examined the correlations among the three measures in seven networks ($n = 49$). There were consistently negative correlations between SE and the other two measures in every network. Notably, the relationship between SD and PLE appeared non-linear in VIS and SMN, showing a second-order polynomial trend, whereas in other networks, the association was more linear but with lower R^2 values. Visual inspection suggested that the observed non-linearity stemmed from an inflection point at PLE = 0 in VIS and SMN for some subjects, indicating a potential transition from blue noise to pink noise. Based on this observation, we hypothesized that the mediation effects of PLE may differ depending on whether PLE values are above or below zero.

To test this hypothesis, we examined how PLE modulates the correlation between SD and SE within simulated data. For this purpose, we generated time series data with different PLE regimes, corresponding to distinct noise types: white noise (PLE = 0), pink noise (PLE = 1), and blue noise (PLE = −1).

White noise (PLE = 0) is characterized by a flat power spectrum, indicating that all frequencies contribute equally, resulting in a highly unstructured and random signal. Pink noise (PLE = 1), in contrast, follows a 1/f power distribution, meaning that lower frequencies dominate, leading to long-range temporal correlations that are commonly observed in biological and cognitive systems. Blue noise (PLE = −1) exhibits the opposite trend, with power increasing at higher frequencies, generating rapid fluctuations with little persistence over time.

As shown in Fig. 5B, in conditions when PLE = −1 (blue noise) or PLE = 0 (white noise), there was no correlation between SD and SE. In contrast, their correlation begins to increase when PLE exceeds 0. Remarkably, this correlation value approaches -1, indicating a fully negative correlation in the presence of pink noise (PLE = 1), which aligns well with our empirical findings.

Together, both empirical data and simulation findings support: (1) the relationship between BOLD SE and SD, and (2) the modulation of their relationship by PLE, which (3) only holds in certain regimes where it relates to pink noise as distinguished from both blue and white noise. This observation underscores the critical role of the PLE in modulating the interaction of BOLD SD and SE, particularly under conditions mimicking biological noise patterns, such as pink noise.

Discussion

The brain-behavior connection is a fundamental question in cognitive neuroscience. Previous research has primarily investigated the neural mechanisms of cognitive processes at high frequencies. However, recent advancements have highlighted the importance of infra-slow frequency dynamics in mediating behavior although the exact mechanisms remain yet unclear. In our study, we provide evidence that three neural dynamic measures—SD, SE, and PLE—are related to behavioral variability, the SD of RT, on an infra-slow timescale in the range of 0.01 to 0.1 Hz.

Notably, we also show that PLE, SD and SE take on distinct roles in mediating brain-behavior connection in our sustained attention task. Specifically, showing in both empirical and simulated data, PLE seems to operate in the neural background from where it mediates the more foreground neural connection of SE and SD as well as the latter's dynamic relationship with the dynamics of the behavior, e.g., SD of RT. That is further supported by our simulation showing a mathematical relationship of SD and SE through their mediation by scale-free dynamics (PLE).

Together, we demonstrate the key relevance of infra-slow dynamics and its distinct features, SE, SD and PLE, in mediating behavioral dynamics along a background-foreground distinction. This sheds light on the key role of the brain's infra-slow dynamics for behavior including its mechanisms that mediate cognitive-behavioral dynamics.

The brain-behavior connection in the infra-slow frequency range

Recent cognitive neuroscience research increasingly emphasizes the importance of large-scale networks in understanding the brain mechanisms underlying human attention[23,82]. Many studies have highlighted the significance of the DMN and the FPN in attention, linking them to the inverse attentional processes involved in attention-demanding tasks[25,72,83,84]. Additionally, the GradCPT study revealed the activation of the DMN, the DAN, and regions within the FPN during tasks, associating these networks with changes in attentional capacity[79].

Our current findings align with these observations while also extending previous research. Notably, our study demonstrates consistent modulation of neural dynamics between rest and task states in the VIS, SMN, DAN, and VAN networks, which are associated with the unimodal cortex. In contrast, within transmodal/high-order networks (including the Limbic network, FPN, and DMN), only SD exhibited task-related changes in the DMN.

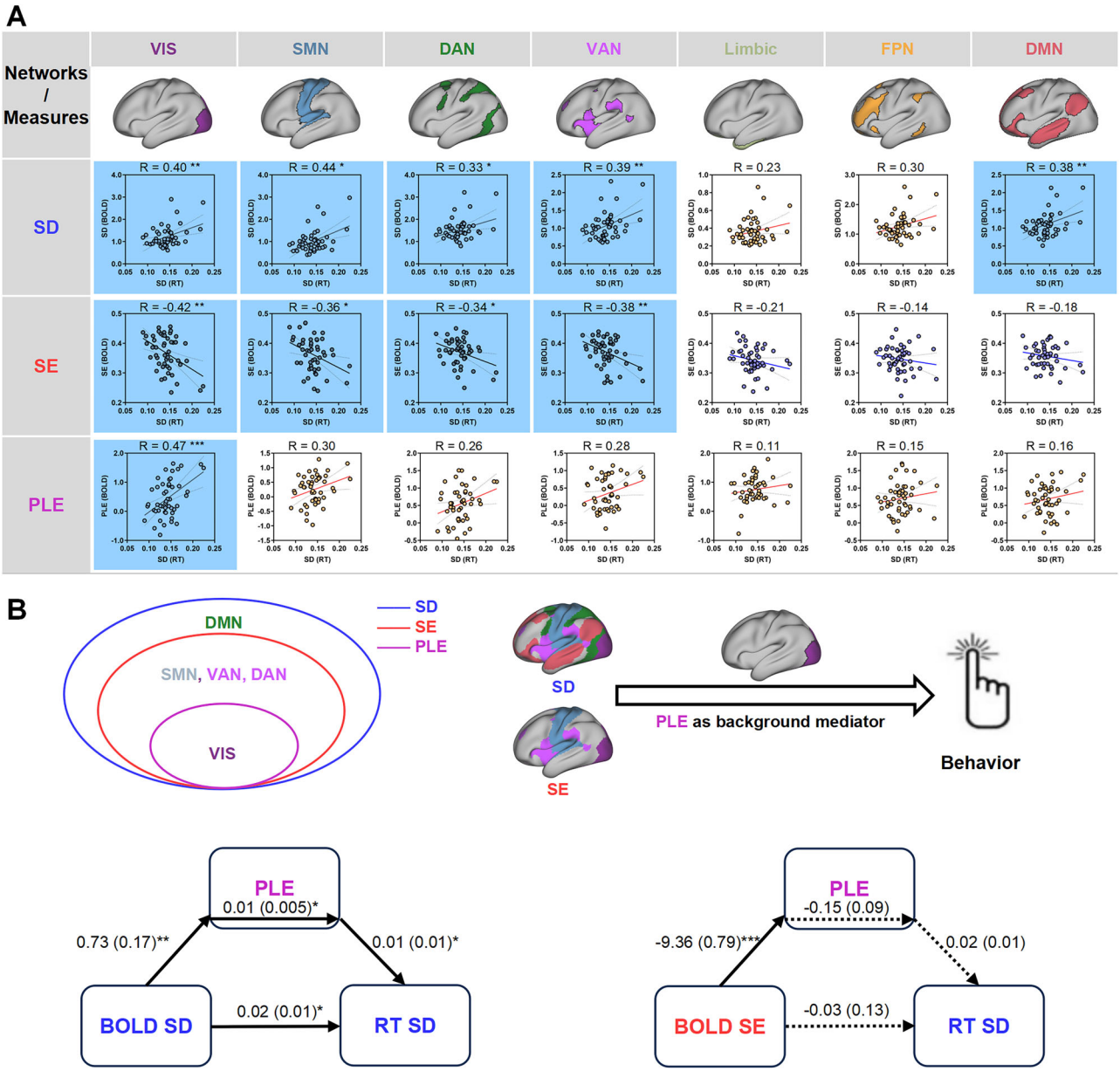

Fig. 4 | BOLD-RT correlation of SD, SE, and PLE at the group level in task state. **A** Pearson correlations for three measures in seven networks. The regression plots with blue-shaded indicate significant correlation ($n = 49$, FDR corrected). **B** The schematics for the hierarchical structure for SD, SE, and PLE. And the mediation model ($n = 49$) for the relationship between BOLD SD/SE and RT SD in task state. Significance levels are denoted as follows: $^{*}p < 0.05$, $^{**}p < 0.01$, $^{***}p < 0.001$, $^{****}p < 0.0001$.

This distinction suggests that while the three dynamic measures (SD, SE, and PLE) follow similar patterns of rest-task modulation in unimodal regions, they diverge in transmodal networks, particularly the DMN.

This divergence may reflect differences in functional specialization between unimodal and transmodal regions. The unimodal cortex primarily processes sensory inputs and motor responses, which are directly engaged by task-related demands, leading to synchronous changes across different measures of neural variability (SD, SE, and PLE). In contrast, transmodal networks, such as the DMN, integrate information across multiple cognitive domains, including internal mentation, memory, and attentional control[84,85]. The fact that only SD exhibited task-related changes in the DMN, while SE and PLE did not, suggests that SD may be more sensitive to cognitive control mechanisms unique to transmodal regions[23], whereas SE and PLE may predominantly reflect background neural dynamics that remain stable in these higher-order networks. Thus, our findings do not simply indicate a dynamic characterization of lower-order visual processing. Instead, they highlight how neural variability differentially tracks changes in brain states depending on the functional role of the network for subsequent behavior—being more homogeneous in unimodal networks but more heterogeneous in transmodal regions.

In line with the rest-task modulation findings, our core discovery is the differentiated roles of neural SD, SE, and PLE in their correlation with behavior. All three measures correlate with behavioral performance but differ across brain networks. We found that SD significantly correlates with behavior in the DMN, while SE does not, consistent with the rest-task difference findings. Additionally, the VIS network showed a significant correlation with RT SD across all three measures. Importantly, the VIS was the only network where RT SD significantly related to the neural PLE, highlighting its role in processing visual inputs in a visually demanding task like ours[86,87].

Notably, both SD and SE exhibited significant behavioral correlations in the SMN, DAN, and VAN, networks specifically involved in sustained

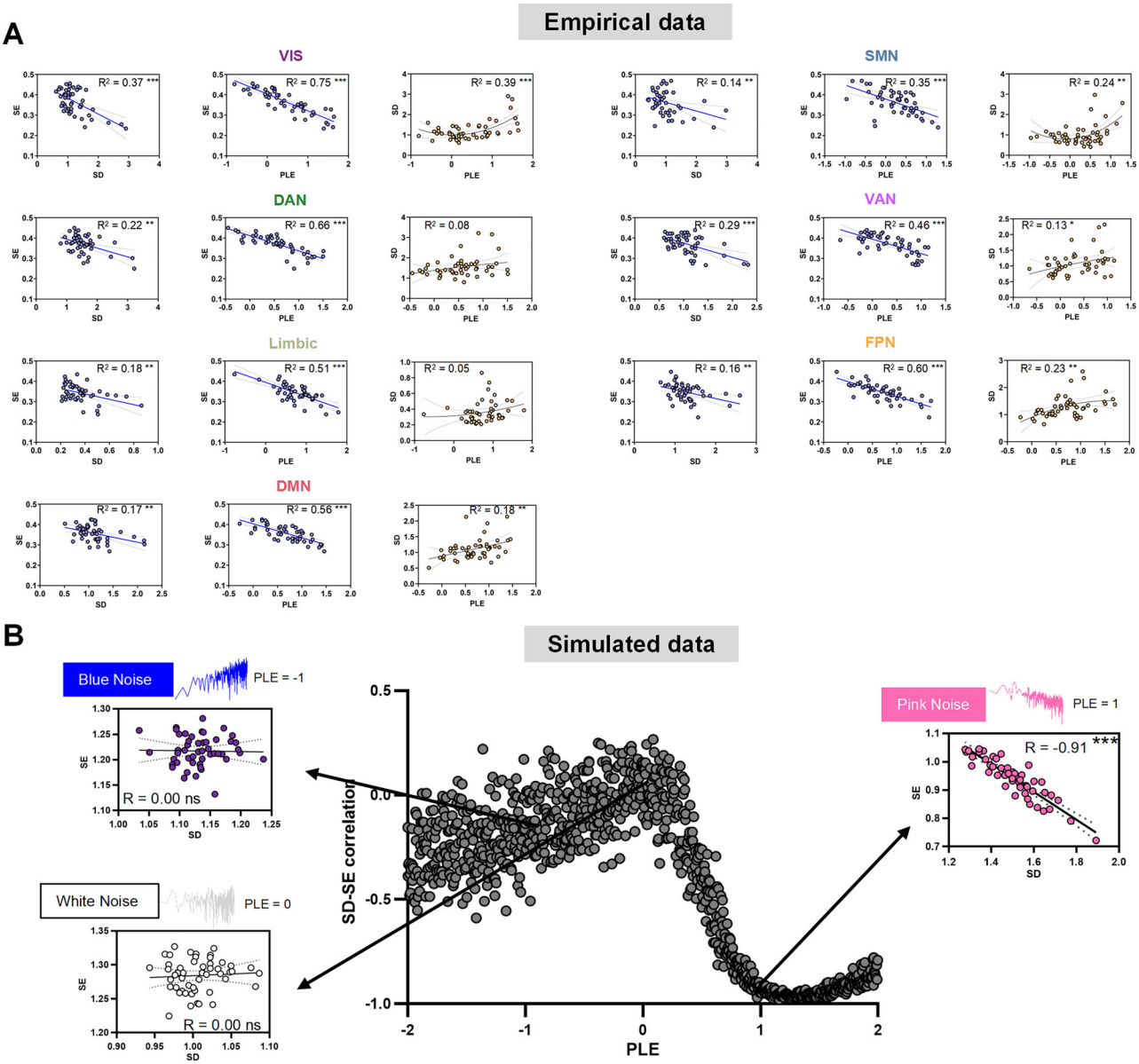

Fig. 5 | PLE as the mediator for brain-behavior and SD-SE relationship. A Correlations between three measures ($n = 49$). **B** The relationship between SD and SE mediated by varying PLE in simulated data. Scatter plots depicted the correlations ($n = 49$) between SD and SE under PLE = -1, 0, and -1.

attention tasks. In contrast, PLE did not show significant behavioral correlations in these networks. This divergence between PLE and SD/SE suggests that PLE functions as a topographic and dynamic background measure, which appears to be less sensitive to specific cognitive-attentional task demands. In other words, while SD and SE reflect task-related fluctuations in brain activity that are closely tied to performance in attention-related tasks, PLE operates more as a general and task-unspecific measure of neural dynamics that is not directly influenced by the specific demands of the task. This distinction in the roles of PLE, SD, and SE is further supported by our other findings, indicating that each measure may capture different aspects of brain dynamics.

Scale-free dynamics regulates the SD-SE and brain-behavior relationship: the main contribution of the low-frequency oscillatory component

To investigate the background role of scale-free dynamics and the differential roles of SD and SE, as well as their relationship, we examined the mediation effect of PLE on the correlation between neural variability and behavioral variability as well as its modulating effects on the purely BOLD correlation of SD and SE. First, we found that PLE significantly mediates the relationship between BOLD SD and behavioral SD but not between BOLD SE and behavioral SD. This suggests again a special role for PLE as distinct from both SD and SE in mediating behavioral dynamics. Moreover, it also implies differential roles of SE and SD, which again further supports our findings of their subtle differences in the networks of their rest-task modulation. Accordingly, our findings strongly indicate differential roles of PLE, SE, and SD in mediating brain-behavior relationship, suggesting a layered-like organization of the brain's neural dynamics in mediating behavioral dynamics[5].

The special role of PLE operating in the neural background is further supported by the purely neuronal, e.g., BOLD relationship of PLE with SE and SD. Our results show that both SD and PLE are negatively correlated with SE, consistent with a previous study[48]. A notable finding is the non-linear relationship between SD and PLE, with an inflection point at approximately PLE = 0. The simulated data further support the results of the non-linear relationship between SD and PLE from real data. During both blue noise (PLE = −1) and white noise (PLE = 0), the correlations between SD and SE are close to zero. In contrast, when PLE increases to 1 (pink

noise), the correlation between SD and SE evolves to a nearly full negative correlation in our simulation just as we observe it in our empirical data: as the signal's scale-free dynamics increases moving from white to pink noise, SD and SE start relating to each other.

The underlying idea is that scale-free dynamics, such as those seen in pink noise, provide a temporal background structure in the neural activity that facilitates the more foreground connection between two distinct aspects of neural variability, SD (which reflects the fluctuation magnitude) and SE (which measures the complexity or entropy). These two measures, which operate on different timescales, become more related with each other in the presence of scale-free dynamics. This connection between SD and SE may thus be mediated by the temporal structure of pink noise which, in turn, plays a key role in linking neural dynamics to behavioral outcomes[48].

While we pointed out the differentiation of distinct layers of neural dynamics, e.g., background and foreground, their relationship to physiological and psychological features remains yet unclear. The PLE is measured across the whole frequency range which renders it a perfect candidate to serve as more global (here understood in a temporal sense in terms of the range of frequencies) background measure. In contrast, cognition and behavior require specific frequencies in both high frequency[8,88] and also within the infra-slow frequency range[78,89]. Together, our findings suggest a topographic-dynamic organization with various layers organized along a gradient from the global brain including all its regions and frequencies/scale-free dynamics (PLE) to more local activity with specific regions and frequencies (SD, SE) specific and restricted regions and frequencies/oscillations (SE, SD) which, in turn, modulates behavior, e.g., SD of RT. That is well in accordance with and supports the recently proposed 'Dynamic layer model of brain' as an integrated dynamic-topographic brain-mind model[5] (see below for details).

Another, though not exclusiv,e perspective is the concept of energy reallocation in PSD, describing the change in the distribution of power in PSD to meet the temporal structure of cognitive tasks[35,76,90]. In the current GradCPT task, subjects were required to respond to ever-changing stimuli that demand sustained attention on a faster timescale. Thus, the specific task shifts the brain signal to a faster timescale to meet the fast-changing input, resulting in a loss of low-frequency energy, explaining the decrease in low-frequency power as well as the PSD. This also partly explains the increased SE in the task state: as the ratio of low/high-frequency power decreases, the details/information in a signal increase[91], which is well compatible with our observation of task-related decreases in PLE and SD accompanied by concurrent SE increase.

The dynamic layer model of the brain: bridging neural activity, cognition, and behavior

Together, both our empirical and simulation findings suggest a background-foreground distinction and organization in the brain's neural dynamics, which is well in line with other empirical findings[32,47], and, on a more theoretical level, with the Dynamic layer model of brain (DLB)[5]. Roughly, the DLB characterizes and defines the brain by the dynamic features of its neural activity that are supposed to be organized along different layers featured by their distinct timescale,s ranging from long to short. This does not mean that the DLB is a purely neural model of the brain, though. The DLB targets a deeper layer of the brain, namely the dynamics of its neural activity and how that, in turn, modulates its cognitive and behavioral function. Such layered dynamical organization of the brain's neural activity distinguishes the DLB from other brain models like the predictive coding model[92] that, rather than on neural activity itself, focus more on the brain's neural function like its cognitive function, and its underlying computational mechanisms.

The results of the present and others[47,93,94] demonstrate clearly how such dynamically- and topographically-layered organization modulates both cognition and behavior as indices of the brain's neural function. The rest-task PLE increase in visual cortex suggests that it plays a key role in the temporal encoding (and processing) of the paradigm's input and its temporal structure, e.g., entrainment[74] and alignment[73] (see also Klar et al. 2023, Wolman et al. 2024 for similar findings). This presents the deepest dynamic layer of the brain. A next layer allows for temporal integration of the various inputs, e.g., trials of the task, over time as possibly mediated by information complexity as measured by SE. That is complemented by yet another layer of neural variability (SD), which provides temporal scaffolding of the output, e.g., the reaction time and its behavioral variability – this is supported by their correlation.

Together, our findings demonstrate three dynamic layers of the brain's neural activity and their respective mechanisms, including (i) scale-free dynamics with temporal input encoding, (ii) information complexity/entropy allowing for temporal input integration, and (iii) neural variability providing temporal scaffolding of the behavioral output and its variability. Reflecting different layers of the brain's neural dynamics, these temporal mechanisms allow connecting input and output through their shared dynamics. This is manifest in the brain's dynamic shaping of its cognition, which stands at the very core of what we recently introduced as "Spatio-temporal Neuroscience"[5,70,95].

Limitations

Several limitations should be noted. Firstly, our experimental paradigm involved behavioral responses in a highly controlled environment with limited dynamics. The human brain operates on multiple timescales, which need to be investigated in natural environments that provide complex inputs aligning with real-world brain function. For instance, music and movie stimuli have been shown to trigger complex brain responses, including changes in functional connectivity. To our knowledge, no study, including our current one, has explored the complex dynamical relationship between brain and behavior across multiple timescales using natural stimuli. Our study may pave the way for investigating the brain-behavior connection on varied timescales.

A critical aspect of our study is the differentiation between fractal and oscillatory properties in the PSD. We focus exclusively on the former, specifically the PLE. While the scale-free nature of the background supports cognitive functions—such as attention in our case—oscillations also play a significant role, particularly when considering the timescale in certain frequency points. These oscillations may serve as a stronger indicator of behavioral variability, as suggested by ref. 96. To date, only a limited number of fMRI studies have examined the oscillatory component within the infra-slow frequency range, such as in the context of aging[40]. However, no research has yet explored its cognitive implications. Further investigation is needed to understand the cognitive relevance of this oscillatory component.

Some methodological considerations should be noted. Firstly, we applied the sample entropy calculation with parameters $m = 2$ and $r = 0.5$. Although these parameters are commonly used and validated by previous studies[48,64,97], further methodological research is necessary to explore the impact of different sample entropy parameters. The parameter m is particularly important as it represents the time length of the mode, which is sensitive to the intrinsic timescale of the data. Furthermore, our analysis focused on the conventional infra-slow frequency range of 0.01–0.1 Hz, which is considered to have a higher signal-to-noise ratio and is less influenced by physiological noise. However, many studies have emphasized that important neural information is also contained in higher frequencies (>0.1 Hz)[3,4]. Future research should investigate these dynamical measures, particularly scale-free dynamics, across a broader frequency range. This approach would provide a more comprehensive understanding of the relationship between brain and behavior across the full spectrum of timescales, from longer to shorter durations.

Conclusion

In the current study, we demonstrated the direct connection of the behavioral dynamics of task performance during sustained attention with the dynamics of the infra-slow frequency BOLD activity. Based on our research, we propose that the temporal dynamics and their relationship to behavior, and more importantly, the layered structure of SD, SE, and PLE, play a pivotal role in organizing the different temporal features of the brain's

task-related processing including its link to behavioral dynamics. This supports the idea that infra-slow frequency scale-free dynamics with its nested faster timescales as a global component[98,99], like the PLE, provides a "neural background" for cognitive function such as sustained attention, serving as a fundamental function for other cognitive functions operating in the foreground[77]. This is well in line with the recently proposed 'Dynamic layer model of brain' (DLB)[5], which, briefly, proposes that the brain's dynamically layered neural activity is instrumental in mediating and shaping behavior and cognition.

Together, our findings emphasize the importance of scale-free dynamics and neural timescales, their spatiotemporal structure, in influencing neural and behavioral dynamics, advancing the understanding of fMRI low-frequency activity and its relation to cognitive functions[70,95]. These findings serve as a catalyst for future research, enabling more nuanced, dynamic, and topographic examinations of infra-slow frequency brain dynamics in brain-behavior connectio,n including its abnormalities in mental disorders.

Methods

Participants and experiment design

The study recruited 49 healthy adult participants at Sichuan Normal University, comprising 24 males and 25 females (age of 21.15 ± 2.10 years). All participants were confirmed to have no psychiatric disorders and were not taking any psychiatric medications. They were required to abstain from alcohol and caffeine for 24 h before the experiment and to maintain regular sleep patterns. The experimental procedures received approval from the Ethics Committee of the Institute of Brain and Psychological Sciences at Sichuan Normal University. All ethical regulations relevant to human research participants were followed.

Participants underwent two scanning sessions: the first session was conducted during resting state, followed by the task state. In the resting state, participants were instructed to lie down, eyes open, with focus on the cross on the center of the screen, and rest without engaging in specific thought processes for 8 min.

The Gradual-onset Continuous Performance Task (GradCPT) paradigm is employed to assess sustained attention (refer to Fig. 1, top-left panel)[100,101]. The GradCPT involved 10 circular grayscale images of urban scenes and an equal number of mountain scenes, standardized in size and grayscale. The task displayed an asymmetrical distribution in GradCPT, with mountain images comprising 10% and urban images 90% of the trials. The sequence of image presentation was randomized to prevent the consecutive display of images from the same category. Transitions between images were achieved by gradually altering their transparency: the outgoing image faded from opaque (0% transparency) to fully transparent (100%), and the incoming image transitioned from fully transparent back to opaque. This fading process lasted for 1200 milliseconds, maintaining constant grayscale and brightness to minimize the potential attentional effects caused by abrupt changes in the stimuli. Participants were tasked with pressing a key using their right thumb when they confidently identified an urban scene and were instructed to refrain from pressing any key upon recognizing a mountain scene. The task comprised 400 trials and spanned 8 min, during which response times and errors were recorded.

fMRI data and preprocessing

Imaging data were acquired using the Siemens 3-T connectome-Skyra scanner at the Brain Imaging Center of Sichuan Normal University. The scanning sequence employed was Gradient-echo EPI, with a repetition time (TR) of 800 milliseconds, echo time of 38 milliseconds, flip angle of 52 degrees, field of view of 208 × 180 mm, slice thickness of 2 mm, 72 slices, and a voxel resolution of 2 x 2 x 2 mm.

The preprocessing of fMRI data was performed using fMRIPrep version 23.0.2 with default settings[102]. The processed data were output in the "fsaverage5" surface format in CIFTI files for subsequent preprocessing and analysis stages. After discarding the initial four time points, we removed artifacts related to six estimated head motion parameters (x, y, z translations and rotations), frame-wise displacement (FD), as well as signals from white matter and cerebrospinal fluid. Finally, we extracted signals corresponding to seven brain networks from the Yeo et al. 2011 template: visual (VIS), somatomotor (SMN), dorsal attention (DAN), ventral attention (VAN), limbic, frontoparietal (FPN), and default-mode (DMN) networks. These signals were then filtered using an ideal filter with a passband of 0.01 Hz to 0.1 Hz.

Behavioral and stimulus confounds control analysis

For each voxel, after performing standard nuisance regression during preprocessing, we applied an additional general linear model (GLM) to account for potential stimulus-related confounds[103]. In this GLM, each stimulus presentation was modeled as an impulse event, convolved with a canonical hemodynamic response function, and included as regressors for three task-related event types: correct omissions, commission errors, and omission errors. We did not regress out correct commission events (accurate responses to non-target city scenes) because their high frequency effectively defined the continuous "task state." All analyses were then repeated on the residual time series from this regression (the "task-regressed" data), and the results are reported in Supplementary Tables 1, 2 and Supplementary Fig. 3. This process is consistent with a previous GradCPT study[104].

Behavioral data and their measures

Response times (RTs) were examined using methods established in previous GradCPT studies[78,79,105]. In the GradCPT paradigm, each image is gradually revealed over a 1200-ms period until it reaches full clarity. Importantly, the transition to the next image begins immediately once an image is fully presented at 1200 ms. RTs were measured from the onset of each image transition. Thus, an RT of exactly 1200 ms indicated a response at the point of full image clarity, without overlap with the following image. RTs shorter than 1200 ms suggested that the participant responded while the image was still transitioning from the previous one. Conversely, RTs longer than 1200 ms showed responses during the transition to the next image. In cases of significantly aberrant RTs (either before 70% clarity of the current image or after 40% clarity of the subsequent image) or multiple responses, we employed an iterative algorithm to optimize the accuracy of recorded responses. Initially, the algorithm allocated clearly correct responses, leaving a minimal number of ambiguous responses (less than 5% of trials).

Ambiguous responses were reassigned to adjacent trials that lacked a recorded response. When two consecutive trials were missing responses, the ambiguous response was allocated to the trial closest in time, except if that trial was a no-go—in which case the absence of a response was treated as a correct omission. If multiple responses occurred within a single trial, only the fastest response was considered valid. In instances where two consecutive trials remained without clear reassignment, the missing RTs for city and mountain scenes were imputed using the median RT for each scene type within that run.

Following these adjustments, we computed the standard deviation (SD) of RTs as an index of sustained cognitive performance, instead of mean of RTs, consistent with previous studies[79,100]. A lower SD reflects more stable response patterns, which are associated with higher vigilance and sustained attention in the GradCPT paradigm. In other words, RT variability reflects fluctuations in attentional stability, whereas the mean RT is primarily influenced by the periodic response to the fixed stimulus interval. This metric has been widely used and replicated in prior studies employing GradCPT to assess cognitive performance, vigilance levels, as well as its neural mechanism[77,104].

The study did not focus on reaction accuracy, where subjects mistakenly responded to mountain images or incorrectly identified city images, as the primary goal was to establish a link between the variability of RT time series and BOLD signals. Hence, error trials were excluded from the time series, and interpolated the missing RT value of these trials by cubic spline interpolation to preserve the time-frequency feature[78]. However, to enhance data transparency in brain-behavior correlation analyses, we reported the results for error trials, including commission errors (responses to mountain

images), omission errors (missed responses to city images), and the mean RTs (Supplementary Tables 4–6).

fMRI data measures

SD. SD is a common metric for evaluating signal variance and has been widely used in fMRI studies. It represents the distributional width of BOLD signals[50]. Previous studies have shown that SD carries important physiological and psychological significance, not merely signal noise[106–108]. In our study, we applied MATLAB's 'std' function to calculate the SD of the BOLD time series for each network and participant.

SE. Sample entropy (SE) is a measure of complexity or regularity, originally developed to assess the unpredictability of fluctuations in time series data[109]. Unlike its predecessor, approximate entropy, SE does not include self-matches, resulting in a more consistent discrimination of complex signals[109,110]. This measure is particularly useful in fMRI studies for evaluating the complexity of neural signals. It functions by identifying repeated patterns; a higher frequency of repetitions indicates more predictable and structured data.

The key parameters used in the calculation of SE were the pattern length m and the similarity factor r. The embedding dimension m was set at 2, which considers pairs of points in constructing the template vectors. The tolerance r, representing the width of the similarity criterion, was set to 0.5 times the standard deviation of the time series.

The formula used for Sample Entropy is:

$$SE(m, r, N) = -\ln\left(\frac{A}{B}\right)$$

where N is the length of the time series, A is the number of matches for templates of length $m + 1$ that remain similar for m points, excluding self-matches, and B is the number of matches for templates of length m. Two patterns match if the distance is less than r. The value setting of m and r is consistent with prior fMRI research[48,64,97]. Our SE calculation script is accessible at http://www.georgnorthoff.com/code.

In sum, higher values of SE indicate greater signal complexity, suggesting less predictable neural activity, whereas lower values denote more predictable neural patterns. Although the use of SE in fMRI data can be criticized due to the thermal noise component in the fMRI signal[111], previous studies have confirmed SE's validity and effectiveness in distinguishing between different brain regions and systems, highlighting its ability to mirror the hierarchical structure and functional diversity of brain systems[48,64].

PLE. The power-law exponent, often denoted as the scaling exponent β, is a critical measure in understanding the temporal scaling properties of time series data[31,34]. To calculate the PLE, we firstly get a power spectral density (PSD) of a time series. Then the log-log plot of the frequency versus power from the PSD was used to determine the power-law relationship. The PLE, represented by the scaling exponent β, corresponds to the negative slope of this log-log plot, as determined by linear regression in log-log space[36,37,48]. This method was utilized, restricting the frequency range to 0.01–0.1 Hz to mitigate interference from scanner drift and physiological noise. Notably, visual inspection (see Fig. 1, schematic for PLE) reveals no apparent oscillatory component within the 0.01–0.1 Hz range, suggesting that the PLE calculation is primarily influenced by the 1/f component. This approach aligns with established methodologies, and our script for calculating PLE is also available at http://www.georgnorthoff.com/code.

The value of the power-law exponent β offers insights into the intrinsic timescale of brain activity. A $\beta = 1$ exponent suggests pink noise, which is typical for many biological systems. In contrast, lower values of β (closer to 0) indicate a flatter spectrum, reflecting more transient and unstructured dynamics. This measure has been linked to shifts in attention, arousal, and pathology-related alterations in brain function[31,36,37,45].

Mediation model analysis

To examine whether the power-law exponent (PLE) mediates the relationship between response time variability (RT SD) and brain signal variability, we conducted a mediation analysis using the CANLAB mediation toolbox for MATLAB[112,113]. Specifically, we tested two mediation models:

1. PLE as a mediator between BOLD signal variability and RT variability:

-The independent variables were the standard deviation (SD) and sample entropy (SE) of BOLD signals during the task.

-The dependent variable was RT SD.

-PLE served as the mediator, allowing us to assess whether neural timescale properties (PLE) explain the link between BOLD signal variability and behavioral variability.

2. PLE as a mediator between different measures of BOLD signal variability:

-The independent variable was the SE of BOLD signals.

-The dependent variable was the SD of BOLD signals.

-PLE was tested as a mediator to evaluate whether infra-slow scale-free dynamics contribute to the relationship between different forms of BOLD variability.

We assessed the significance of direct and indirect effects using a bootstrapping approach with 10,000 resampled iterations, generating 95% confidence intervals. This allowed us to determine whether the mediation effects were statistically robust.

Simulation analysis

To investigate the mathematical relationship between SD and SE under varying PLE, we generated 1000 samples of colored noise consistent with different PLE values. This simulation utilized MATLAB's built-in function "dsp.ColoredNoise," covering PLE values ranging from -2 to 2 at equal intervals. Both SD and SE were calculated in these simulations to explore how PLE influences their relationship.

Statistics and reproducibility

A significance threshold of $p < 0.05$ was applied for all two-sided statistical tests. Sample sizes are reported in the main text. The statistical methods and multiple comparison correction procedures are detailed below.

Difference analysis: We conducted difference analyses using paired t-tests for SD, SE, and PLE of BOLD signals. These analyses encompassed comparisons between rest and task state and the z-scores of the three measures in task state across seven networks.

Behavior-brain correlation analysis: To investigate the relationship between behavioral variability and three BOLD measures, we performed Pearson's correlation analyses: (1) For each subject, we extracted one behavioral measure (RT SD) and three BOLD measures (SD, SE, and PLE) within each of the seven networks. (2) We then computed Pearson's correlations between RT SD and each of the three BOLD measures within each network, yielding a group-level behavior-brain correlation for each network. (3) Additionally, Pearson's correlations were computed among the three BOLD measures within both empirical data and simulated data (Fig. 4).

Three BOLD measures correlations: To assess the relationships between SD, SE, and PLE, we initially computed Pearson's correlations. However, given that visual inspection of scatter plots suggested non-linear trends, particularly in VIS and SMN, we also performed polynomial regression analyses to better capture these relationships. Specifically, we fitted second-order polynomial models and compared their R^2 values to those of linear models. This approach allowed us to determine whether non-linear relationships were more appropriate for specific networks.

Multiple comparison correction: Statistical tests (21 analyses across seven networks and three measures—SD, SE, and PLE; seven networks × three BOLD measures) were corrected for false discovery rate (FDR) using the linear step-up procedure introduced by ref. 114.

Reporting summary

Further information on research design is available in the Nature Portfolio Reporting Summary linked to this article.

Data availability

The fMRI dataset assessed in this analysis is available from the corresponding author upon reasonable request. The source data behind the graphs in the paper can be found in Supplementary Data 1.

Code availability

The code for replicating the calculations of the three key measures (SD, SE, and PLE) is publicly available on our website: https://www.georgnorthoff.com/code.

Received: 7 November 2024; Accepted: 26 June 2025;
Published online: 16 July 2025

References

1. Golesorkhi, M., Gomez-Pilar, J., Tumati, S., Fraser, M. & Northoff, G. Temporal hierarchy of intrinsic neural timescales converges with spatial core-periphery organization. *Commun. Biol.* **4**, 277 (2021).
2. Palva, S. & Palva, J. M. Roles of brain criticality and multiscale oscillations in temporal predictions for sensorimotor processing. *Trends Neurosci.* **41**, 729–743 (2018).
3. Buzsáki, G. & Draguhn, A. Neuronal oscillations in cortical networks. *Science* **304**, 1926–1929 (2004).
4. Zuo, X. N. et al. The oscillating brain: Complex and reliable. *Neuroimage* **49**, 1432–1445 (2010).
5. Northoff, G. *From Brain Dynamics to the Mind: Spatiotemporal Neuroscience* (Elsevier, 2024).
6. Helfrich, R. F. et al. Neural mechanisms of sustained attention are rhythmic. *Neuron* **99**, 854–865.e855 (2018).
7. Klimesch, W., Sauseng, P. & Hanslmayr, S. EEG alpha oscillations: the inhibition-timing hypothesis. *Brain Res. Rev.* **53**, 63–88 (2007).
8. Hua, J. et al. Alpha and theta peak frequency track on-and off-thoughts. *Commun. Biol.* **5**, 209 (2022).
9. Adaikkan, C. et al. Gamma entrainment binds higher-order brain regions and offers neuroprotection. *Neuron* **102**, 929–943 (2019).
10. Scheeringa, R. et al. Neuronal dynamics underlying high-and low-frequency EEG oscillations contribute independently to the human BOLD signal. *Neuron* **69**, 572–583 (2011).
11. Hacker, C. D., Snyder, A. Z., Pahwa, M., Corbetta, M. & Leuthardt, E. C. Frequency-specific electrophysiologic correlates of resting state fMRI networks. *Neuroimage* **149**, 446–457 (2017).
12. Das, A., Murphy, K. & Drew, P. J. Rude mechanicals in brain haemodynamics: non-neural actors that influence blood flow. *Philos. Trans. R. Soc. Lond. B Biol. Sci.* **376**, 20190635 (2021).
13. Gong, Z.-Q. & Zuo, X.-N. Dark brain energy: toward an integrative model of spontaneous slow oscillations. *Phys. Life Rev.* **52**, 278–297 (2025).
14. Pan, W.-J., Thompson, G. J., Magnuson, M. E., Jaeger, D. & Keilholz, S. Infraslow LFP correlates to resting-state fMRI BOLD signals. *Neuroimage* **74**, 288–297 (2013).
15. Lu, H. et al. Low-but not high-frequency LFP correlates with spontaneous BOLD fluctuations in rat whisker barrel cortex. *Cereb. Cortex* **26**, 683–694 (2016).
16. Hiltunen, T. et al. Infra-slow EEG fluctuations are correlated with resting-state network dynamics in fMRI. *J. Neurosci.* **34**, 356–362 (2014).
17. Palva, J. M. & Palva, S. Infra-slow fluctuations in electrophysiological recordings, blood-oxygenation-level-dependent signals, and psychophysical time series. *Neuroimage* **62**, 2201–2211 (2012).
18. Turchi, J. et al. The basal forebrain regulates global resting-state fMRI fluctuations. *Neuron* **97**, 940–952 (2018).
19. Gutierrez-Barragan, D., Basson, M. A., Panzeri, S. & Gozzi, A. Infraslow state fluctuations govern spontaneous fMRI network dynamics. *Curr. Biol.* **29**, 2295–2306 (2019).
20. Ao, Y., Catal, Y., Lechner, S., Hua, J. & Northoff, G. Intrinsic neural timescales relate to the dynamics of infraslow neural waves. *Neuroimage* **285**, 120482 (2024).
21. Ao, Y. et al. Spatiotemporal dedifferentiation of the global brain signal topography along the adult lifespan. *Hum. Brain Mapp.* **44**, 5906–5918 (2023).
22. Sasai, S. et al. Frequency-specific task modulation of human brain functional networks: A fast fMRI study. *Neuroimage* **224**, 117375 (2021).
23. Zhang, H. et al. Default mode network mediates low-frequency fluctuations in brain activity and behavior during sustained attention. *Hum. Brain Mapp.* **43**, 5478–5489 (2022).
24. Hanslmayr, S., Gross, J., Klimesch, W. & Shapiro, K. L. The role of alpha oscillations in temporal attention. *Brain Res. Rev.* **67**, 331–343 (2011).
25. Fiebelkorn, I. C. & Kastner, S. A rhythmic theory of attention. *Trends Cogn. Sci.* **23**, 87–101 (2019).
26. Huk, A., Bonnen, K. & He, B. J. Beyond trial-based paradigms: Continuous behavior, ongoing neural activity, and natural stimuli. *J. Neurosci.* **38**, 7551–7558 (2018).
27. Marom, S. Neural timescales or lack thereof. *Prog. Neurobiol.* **90**, 16–28 (2010).
28. Golesorkhi, M. et al. The brain and its time: intrinsic neural timescales are key for input processing. *Commun. Biol.* **4**, 970 (2021).
29. Wolman, A. et al. Intrinsic neural timescales mediate the cognitive bias of self–temporal integration as key mechanism. *NeuroImage* **268**, 119896 (2023).
30. Manea, A. M. et al. Neural timescales reflect behavioral demands in freely moving rhesus macaques. *Nat. Commun.* **15**, 2151 (2024).
31. He, B. J. Scale-free brain activity: past, present, and future. *Trends Cogn. Sci.* **18**, 480–487 (2014).
32. Fuscà, M. et al. Brain criticality predicts individual levels of inter-areal synchronization in human electrophysiological data. *Nat. Commun.* **14**, 4736 (2023).
33. Linkenkaer-Hansen, K., Nikouline, V. V., Palva, J. M. & Ilmoniemi, R. J. Long-range temporal correlations and scaling behavior in human brain oscillations. *J. Neurosci.* **21**, 1370–1377 (2001).
34. He, B. J. Scale-free properties of the functional magnetic resonance imaging signal during rest and task. *J. Neurosci.* **31**, 13786–13795 (2011).
35. Wang, Y. et al. Multiscale energy reallocation during low-frequency steady-state brain response. *Hum. Brain Mapp.* **39**, 2121–2132 (2018).
36. Klar, P., Çatal, Y., Langner, R., Huang, Z. & Northoff, G. Scale-free dynamics in the core-periphery topography and task alignment decline from conscious to unconscious states. *Commun. Biol.* **6**, 499 (2023).
37. Klar, P., Çatal, Y., Langner, R., Huang, Z. & Northoff, G. Scale-free dynamics of core-periphery topography. *Hum. Brain Mapp.* **44**, 1997–2017 (2023).
38. Huntenburg, J. M., Bazin, P. L. & Margulies, D. S. Large-scale gradients in human cortical organization. *Trends Cogn. Sci.* **22**, 21–31 (2018).
39. Golesorkhi, M. et al. From temporal to spatial topography: hierarchy of neural dynamics in higher-and lower-order networks shapes their complexity. *Cereb. Cortex* **32**, 5637–5653 (2022).
40. Ao, Y. et al. The temporal dedifferentiation of global brain signal fluctuations during human brain ageing. *Sci. Rep.* **12**, 3616 (2022). Article.
41. Kasagi, M. et al. Association between scale-free brain dynamics and behavioral performance: Functional MRI study in resting state and face processing task. *Behav. Neurol.* **2017**, 2824615 (2017).
42. Huang, Z. et al. Is there a nonadditive interaction between spontaneous and evoked activity? Phase-dependence and its relation to the temporal structure of scale-free brain activity. *Cereb. Cortex* **27**, 1037–1059 (2017).

43. Scalabrini, A. et al. Spontaneous brain activity predicts task-evoked activity during animate versus inanimate touch. *Cereb. Cortex* **29**, 4628–4645 (2019).
44. Palva, J. M., Zhigalov, A., Hirvonen, J., Korhonen, O., Linkenkaer-Hansen, K. & Palva, S. Neuronal long-range temporal correlations and avalanche dynamics are correlated with behavioral scaling laws. *Proc. Natl. Acad. Sci. USA*. **110**, 3585–3590 (2013).
45. Jones, S. A., Barfield, J. H., Norman, V. K. & Shew, W. L. Scale-free behavioral dynamics directly linked with scale-free cortical dynamics. *Elife* **12**, e79950 (2023).
46. Northoff, G., Buccellato, A. & Zilio, F. Connecting brain and mind through temporo-spatial dynamics: Towards a theory of common currency. *Phys. life Rev.* **52**, 29–43 (2024).
47. Wolman, A., Çatal, Y., Klar, P., Steffener, J. & Northoff, G. Repertoire of timescales in uni–and transmodal regions mediate working memory capacity. *NeuroImage* **291**, 120602 (2024).
48. Çatal, Y., Gomez-Pilar, J. & Northoff, G. Intrinsic dynamics and topography of sensory input systems. *Cereb. Cortex* **32**, 4592–4604 (2022).
49. Wolff, A. et al. Intrinsic neural timescales: temporal integration and segregation. *Trends Cogn. Sci.* **26**, 159–173 (2022).
50. Waschke, L., Kloosterman, N. A., Obleser, J. & Garrett, D. D. Behavior needs neural variability. *Neuron* **109**, 751–766 (2021).
51. Guitart-Masip, M. et al. BOLD variability is related to dopaminergic neurotransmission and cognitive aging. *Cereb. Cortex* **26**, 2074–2083 (2016).
52. Armbruster-Genç, D. J., Ueltzhöffer, K. & Fiebach, C. J. Brain signal variability differentially affects cognitive flexibility and cognitive stability. *J. Neurosci.* **36**, 3978–3987 (2016).
53. Wong, C. W., DeYoung, P. N. & Liu, T. T. Differences in the resting-state fMRI global signal amplitude between the eyes open and eyes closed states are related to changes in EEG vigilance. *Neuroimage* **124**, 24–31 (2016).
54. Wong, C. W., Olafsson, V., Tal, O. & Liu, T. T. The amplitude of the resting-state fMRI global signal is related to EEG vigilance measures. *Neuroimage* **83**, 983–990 (2013).
55. Huang, Z. et al. Decoupled temporal variability and signal synchronization of spontaneous brain activity in loss of consciousness: an fMRI study in anesthesia. *Neuroimage* **124**, 693–703 (2016).
56. Takahashi, T. et al. Enhanced brain signal variability in children with autism spectrum disorder during early childhood. *Hum. Brain Mapp.* **37**, 1038–1050 (2016).
57. Li, L. et al. Altered brain signal variability in patients with generalized anxiety disorder. *Front Psychiatry* **10**, 84 (2019).
58. Grady, C. L. & Garrett, D. D. Understanding variability in the BOLD signal and why it matters for aging. *Brain Imaging Behav.* **8**, 274–283 (2014).
59. Garrett, D. D., Kovacevic, N., McIntosh, A. R. & Grady, C. L. The importance of being variable. *J. Neurosci.* **31**, 4496–4503 (2011).
60. Garrett, D. D. et al. Moment-to-moment brain signal variability: A next frontier in human brain mapping?. *Neurosci. Biobehav. Rev.* **37**, 610–624 (2013).
61. Grady, C. L. & Garrett, D. D. Brain signal variability is modulated as a function of internal and external demand in younger and older adults. *NeuroImage* **169**, 510–523 (2018).
62. Xie, W. et al. Age-related changes in the association of resting-state fMRI signal variability and global functional connectivity in non-demented healthy people. *Psychiatry Res* **291**, 113257 (2020).
63. Shannon, C. E. A mathematical theory of communication. *Bell Syst. Tech. J.* **27**, 379–423 (1948).
64. Omidvarnia, A., Zalesky, A., Van De Ville, D., Jackson, G. D. & Pedersen, M. Temporal complexity of fMRI is reproducible and correlates with higher order cognition. *NeuroImage* **230**, 117760 (2021).
65. Wang, Y. et al. Spatial variability of low frequency brain signal differentiates brain states. *PLoS One* **15**, e0242330 (2020).
66. Wang, Y. et al. Spatial complexity of brain signal is altered in patients with generalized anxiety disorder. *J. Affect. Disord.* **246**, 387–393 (2019).
67. Nezafati, M., Temmar, H. & Keilholz, S. D. Functional MRI signal complexity analysis using sample entropy. *Front. Neurosci.* **14**, 700 (2020).
68. Jia, Y., Gu, H. & Luo, Q. Sample entropy reveals an age-related reduction in the complexity of dynamic brain. *Sci. Rep.* **7**, 7990 (2017).
69. Sokunbi, M. O. et al. Resting state fMRI entropy probes complexity of brain activity in adults with ADHD. *Psychiatry Res.: Neuroimaging* **214**, 341–348 (2013).
70. Northoff, G., Wainio-Theberge, S. & Evers, K. Is temporo-spatial dynamics the “common currency” of brain and mind? In Quest of “Spatiotemporal Neuroscience. *Phys. Life Rev.* **33**, 34–54 (2020).
71. Ding, N., Melloni, L., Zhang, H., Tian, X. & Poeppel, D. Cortical tracking of hierarchical linguistic structures in connected speech. *Nat. Neurosci.* **19**, 158–164 (2016).
72. Clayton, M. S., Yeung, N. & Kadosh, R. C. The roles of cortical oscillations in sustained attention. *Trends Cogn. Sci.* **19**, 188–195 (2015).
73. Northoff, G., Klar, P., Bein, M. & Safron, A. As without, so within: how the brain’s temporo-spatial alignment to the environment shapes consciousness. *Interface Focus* **13**, 20220076 (2023).
74. Lakatos, P., Gross, J. & Thut, G. A new unifying account of the roles of neuronal entrainment. *Curr. Biol.* **29**, R890–R905 (2019).
75. Wang, Y. et al. Steady-state BOLD response modulates low frequency neural oscillations. *Sci. Rep.* **4**, 7376 (2014).
76. Wang, Y. et al. Low frequency steady-state brain responses modulate large scale functional networks in a frequency-specific means. *Hum. Brain Mapp.* **37**, 381–394 (2016).
77. Esterman, M. & Rothlein, D. Models of sustained attention. *Curr. Opin. Psychol.* **29**, 174–180 (2019).
78. Qiao, J. et al. The infraslow frequency oscillatory transcranial direct current stimulation over the left dorsolateral prefrontal cortex enhances sustained attention. *Front. Aging Neurosci.* **14**, 879006 (2022).
79. Esterman, M., Noonan, S. K., Rosenberg, M. & DeGutis, J. In the zone or zoning out? Tracking behavioral and neural fluctuations during sustained attention. *Cereb. Cortex* **23**, 2712–2723 (2013).
80. Margulies, D. S. et al. Situating the default-mode network along a principal gradient of macroscale cortical organization. *Proc. Natl. Acad. Sci. USA* **113**, 12574–12579 (2016).
81. Vossel, S., Geng, J. J. & Fink, G. R. Dorsal and ventral attention systems: distinct neural circuits but collaborative roles. *Neuroscientist* **20**, 150–159 (2014).
82. Fox, M. D. et al. The human brain is intrinsically organized into dynamic, anticorrelated functional networks. *Proc. Natl. Acad. Sci. USA* **102**, 9673–9678 (2005).
83. Andrews-Hanna, J. R., Reidler, J. S., Huang, C. & Buckner, R. L. Evidence for the default network’s role in spontaneous cognition. *J. Neurophysiol.* **104**, 322–335 (2010).
84. Buckner, R. L. & DiNicola, L. M. The brain’s default network: updated anatomy, physiology and evolving insights. *Nat. Rev. Neurosci.* **20**, 593–608 (2019).
85. Cheng, X. J., Yuan, Y., Wang, Y. H. & Wang, R. B. Neural antagonistic mechanism between default-mode and task-positive networks. *Neurocomputing* **417**, 74–85 (2020).

86. Beltramo, R. & Scanziani, M. A collicular visual cortex: Neocortical space for an ancient midbrain visual structure. *Science* **363**, 64–69 (2019).
87. Kastner, S. & Ungerleider, L. G. Mechanisms of visual attention in the human cortex. *Annu Rev. Neurosci.* **23**, 315–341 (2000).
88. Busch, N. A., Dubois, J. & VanRullen, R. The phase of ongoing EEG oscillations predicts visual perception. *J. Neurosci.* **29**, 7869–7876 (2009).
89. Wang, Y. et al. Low-frequency phase-locking of brain signals contribute to efficient face recognition. *Neuroscience* **422**, 172–183 (2019).
90. Wang, Y. et al. Steady-state BOLD response to higher-order cognition modulates low frequency neural oscillations. *J. Cogn. Neurosci.* **27**, 2406–2415 (2015).
91. Koverda, V. & Skokov, V. Maximum entropy in a nonlinear system with a 1/f power spectrum. *Phys. A: Stat. Mech. Appl.* **391**, 21–28 (2012).
92. Friston, K. The free-energy principle: a unified brain theory?. *Nat. Rev. Neurosci.* **11**, 127–138 (2010).
93. Wolman, A., Lechner, S., Angeletti, L. L., Goheen, J. & Northoff, G. From the brain's encoding of input dynamics to its behavior: neural dynamics shape bias in decision making. *Commun. Biol.* **7**, 1538 (2024).
94. Chuipka, N., Smy, T. & Northoff, G. From neural activity to behavioral engagement: temporal dynamics as their "common currency" during music. *NeuroImage* **312**, 121209 (2025).
95. Northoff, G., Wainio-Theberge, S. & Evers, K. Spatiotemporal Neuroscience – what is it and why we need it. *Phys. Life Rev.* **33**, 78–87 (2020).
96. Wainio-Theberge, S., Wolff, A., Gomez-Pilar, J., Zhang, J. & Northoff, G. Variability and task-responsiveness of electrophysiological dynamics: scale-free stability and oscillatory flexibility. *NeuroImage* **256**, 119245 (2022).
97. McDonough, I. M. & Nashiro, K. Network complexity as a measure of information processing across resting-state networks: evidence from the Human Connectome Project. *Front. Hum. Neurosci.* **8**, 409 (2014).
98. Buzsáki, G. *Rhythms of the brain*. (Oxford University Press, 2006).
99. Northoff, G. & Zilio, F. Temporo-spatial Theory of Consciousness (TTC) - Bridging the gap of neuronal activity and phenomenal states. *Behav. Brain Res.* **424**, 113788 (2022).
100. Rosenberg, M., Noonan, S., DeGutis, J. & Esterman, M. Sustaining visual attention in the face of distraction: a novel gradual-onset continuous performance task. *Atten., Percept. Psychophys.* **75**, 426–439 (2013).
101. Rosenberg, M. D. et al. A neuromarker of sustained attention from whole-brain functional connectivity. *Nat. Neurosci.* **19**, 165–171 (2016).
102. Esteban, O. et al. fMRIPrep: a robust preprocessing pipeline for functional MRI. *Nat. Methods* **16**, 111–116 (2019).
103. Fair, D. A. et al. A method for using blocked and event-related fMRI data to study "resting state" functional connectivity. *Neuroimage* **35**, 396–405 (2007).
104. Fortenbaugh, F. C., Rothlein, D., McGlinchey, R., DeGutis, J. & Esterman, M. Tracking behavioral and neural fluctuations during sustained attention: A robust replication and extension. *NeuroImage* **171**, 148–164 (2018).
105. Esterman, M., Reagan, A., Liu, G., Turner, C. & DeGutis, J. Reward reveals dissociable aspects of sustained attention. *J. Exp. Psychol.: Gen.* **143**, 2287 (2014).
106. Stein, R. B., Gossen, E. R. & Jones, K. E. Neuronal variability: noise or part of the signal?. *Nat. Rev. Neurosci.* **6**, 389–397 (2005).
107. Uddin, L. Q. Bring the noise: reconceptualizing spontaneous neural activity. *Trends Cogn. Sci.* **24**, 734–746 (2020).
108. Dinstein, I., Heeger, D. J. & Behrmann, M. Neural variability: friend or foe?. *Trends Cogn. Sci.* **19**, 322–328 (2015).
109. Richman, J. S. & Moorman, J. R. Physiological time-series analysis using approximate entropy and sample entropy. *Am. J. Physiol. -Heart Circ. Physiol.* **278**, H2039–H2049 (2000).
110. Cieri, F., Zhuang, X., Caldwell, J. Z. & Cordes, D. Brain entropy during aging through a free energy principle approach. *Front. Hum. Neurosci.* **15**, 647513 (2021).
111. Liu, T. T. Noise contributions to the fMRI signal: An overview. *NeuroImage* **143**, 141–151 (2016).
112. Shrout, P. E. & Bolger, N. Mediation in experimental and nonexperimental studies: new procedures and recommendations. *Psychol. methods* **7**, 422 (2002).
113. Wager, T. D., Davidson, M. L., Hughes, B. L., Lindquist, M. A. & Ochsner, K. N. Prefrontal-subcortical pathways mediating successful emotion regulation. *Neuron* **59**, 1037–1050 (2008).
114. Benjamini, Y. & Hochberg, Y. Controlling the false discovery rate: a practical and powerful approach to multiple testing. *J. R. Stat. Soc.: Ser. B (Methodol.)* **57**, 289–300 (1995).

Acknowledgements

This research was funded by the European Union's Horizon 2020 Framework Program for Research and Innovation under the Specific Grant Agreement No. 785907 (Human Brain Project SGA2). Y.A. is grateful for the support from the China Scholarship Council (202208510069). Data collection was supported by Y.W. through the National Science Foundation of China (62177035, 32471101). G.N. acknowledges funding from UMRF, uOBMRI, CIHR, and PSI. Additionally, we appreciate the tri-council grant from the Canada–UK Artificial Intelligence (AI) Initiative, supported by CIHR, NSERC, and SSHRC, for the project 'The self as agent–environment nexus: crossing disciplinary boundaries to help human selves and anticipate artificial selves' (ES/T01279X/1) in collaboration with Karl J. Friston from the UK.

Author contributions

Y.A. designed the research, conducted data analysis, prepared the figures, and wrote the manuscript. P.K. and Y.C. contributed to coding, methodology, and manuscript editing and review. Y.W. was responsible for experimental design and data collection. G.N. provided invaluable guidance and supervision throughout the research.

Competing interests

The authors declare that the research was conducted in the absence of any commercial or financial relationships that could be construed as a potential conflict of interest.

Additional information

Supplementary information The online version contains supplementary material available at https://doi.org/10.1038/s42003-025-08448-3.

Correspondence and requests for materials should be addressed to Yifeng Wang or Georg Northoff.

Peer review information *Communications Biology* thanks Shira Baror and the other, anonymous, reviewer(s) for their contribution to the peer review of this work.